Analytical Prediction of Self-organized Traffic Jams as a Function of Increasing ACC Penetration

Kshitij Jerath and Sean N. Brennan

***Abstract*— Self-organizing traffic jams are known to occur in medium-to-high density traffic flows and it is suspected that Adaptive Cruise Control (ACC) may affect their onset in mixed human-ACC traffic. Unfortunately, closed-form solutions that predict the occurrence of these jams in mixed human-ACC traffic do not exist. In this paper, both human and ACC driving behaviors are modeled using the General Motors' fourth car-following model and are distinguished by using different model parameter values. A closed-form solution that explains the impact of ACC on congestion due to the formation of self-organized traffic jams (or "phantom" jams) is presented. The solution approach utilizes the master equation for modeling the self-organizing behavior of traffic flow at a mesoscopic scale, and the General Motors' fourth car-following model for describing the driver behavior at the microscopic scale. It is found that while introduction of ACC-enabled vehicles into the traffic stream may produce higher traffic flows, it also results in disproportionately higher susceptibility of the traffic flow to congestion.**

***Index Terms* — Cruise Control, Intelligent Vehicles, Self-organization, Traffic Flow.**

I. Introduction

The US Department of Transportation stated in a recent report that "between 1985 and 2006, vehicle miles traveled increased by nearly 100 percent, while highway lane miles only increased 5 percent during the same period" [1]. Another report from the Texas Transportation Institute mentioned that "between 1982 and 2005, the percentage of the major road system that is congested grew from 29 percent to 48 percent" [2]. These data indicate an increasing mismatch between highway capacity and vehicular population, and suggest a need to study and provide countermeasures to alleviate traffic congestion. Recent studies have shown that traffic jams on highways may be *self-organized*, i.e. vehicle clusters may spontaneously emerge from initially homogeneous traffic if the vehicle density exceeds a critical value [3]. Such spontaneously-formed vehicle clusters or traffic jams have no apparent root causes (such as an accident) and are often referred to as "phantom" jams [4]. Self-organized traffic jams may lead to adverse effects on the environment in terms of excessive emissions, financial losses in terms of fuel wastage and losses in productivity in terms of lost man hours.

The recent advent of Adaptive Cruise Control (ACC) technologies in mainstream vehicles holds the potential to significantly alter traffic flow dynamics and affect the formation of traffic jams. This paper addresses the question of how an increase in penetration of ACC-enabled vehicles in highway traffic alters the dynamics of self-organizing traffic jams. Specifically, the effect of ACC penetration rate on critical vehicle density is examined for traffic flow on a closed ring road. The investigation of traffic flow on a closed ring road makes the analysis amenable to the derivation of a closed-form analytical solution by avoiding unwieldy open boundary conditions such as on- and off-ramps encountered on typical roads. A closed-form analytical solution helps simplify the study of the impact of increased ACC penetration on traffic flow and provides a much-needed analysis tool that is well supplemented by existing approaches which utilize numerical simulations or experimental data. Section 2 of the paper provides an overview of existing research on the impact of ACC on traffic flow and congestion. Section 3 discusses a master equation approach for modeling self-organized traffic jams developed by Mahnke [5]. Section 4 develops this approach further to incorporate cruise control algorithms into the analysis framework. Section 5 examines the analytical results based on different penetration levels of ACC-enabled vehicles in traffic flow. Section 6 discusses the findings from numerical simulations used to validate the obtained analytical results. Section 7 summarizes the results obtained from this work.

II. Literature Review

Active research has been performed in the area of adaptive cruise control and car-following driver models by Herman, Gazis and Potts [6], Seiler, Pant and Hedrick [7], Darbha [8], Zhou and Peng [9], Ioannou [10], Helbing, Treiber and Kesting [11], and Barooah, Mehta and Hespanha [12]. These studies have suggested various methods for designing car-following or cruise control algorithms. While some of these studies [7], [8], [9] present analytical results pertaining to the impact of specific cruise control algorithms on string stability and traffic flow stability, they are predominantly focused on

Manuscript received December 20, 2011. The authors are with the Department of Mechanical and Nuclear Engineering at The Pennsylvania State University, University Park, PA 16802, USA (Corresponding author: phone: 814-863-2430; fax: 814-865-9693; e-mail: sbrennan@ psu.edu (Sean N. Brennan)).

single species environments, i.e. traffic flows with only one type of driver. In cases where analytical results for multi-species (or mixed traffic flow) environments are presented [10], the analysis is limited to specific lead vehicle maneuvers and pertains only to string stability of platoons. Further, the analysis approaches presented in these studies [6], [7], [12] are not easily extended to a multi-species environment representative of a real-life traffic flow, where ACC-enabled and human-driven vehicles may be randomly positioned in the traffic stream.

Other studies that analyze the impact of automated vehicle systems on traffic flows representative of real-life situations have also been performed in recent times [13], [14]. Unfortunately, most such studies are based on numerical simulations and do not present analytical results detailing the impact of the introduction of ACC-enabled vehicles on traffic congestion. Different studies based on systems of mixed ACC-enabled and human-driven vehicular traffic suggest that traffic flow may either increase or decrease [13]. Since there isn't a clear mandate on the impact of introduction of ACC-enabled vehicles into highway traffic, an urgent need exists to analyze their effect.

Active research has also been performed to better understand traffic flow dynamics by Daganzo [15], [16], Helbing and Treiber [17], [18], [19], and Jerath and Brennan [20]. Specifically, active research has been performed to study the phenomenon of self-organized traffic jams by Kerner and Konhäuser [3], Nagel and Paczuski [21], and Mahnke, Kaupužs, Lubashevsky, Pieret, Kühne and Frishfelds [5], [22], [23], [24]. Most existing methodologies for analyzing traffic flow are based primarily on either macroscopic [3], [12], [15] or microscopic models [11] [17] [21]. Macroscopic models are not conducive for analyzing traffic comprising a mixture of ACC-enabled and human-driven vehicles, while microscopic models rely primarily on numerical simulations and cannot be solved analytically for a large number of vehicles. Further, self-organized traffic jams form at a scale that is between the macroscopic (traffic stream) and microscopic (individual vehicle) scales, and thus a mesoscopic ('meso-', Greek for middle) approach is required to analyze their behavior. Recent advances by Mahnke [5] [23] in modeling the mesoscopic behavior of traffic provide new opportunities for such analysis. However, most studies on clustering or aggregative behavior have been focused on physical systems [25] and little research has been done to analytically study the impact of ACC on the formation of self-organized traffic jams at a mesoscopic scale. Further, as mentioned earlier, other studies regarding the impact of ACC on traffic flows representative of real-life situations have primarily relied on numerical simulations [11], [14], [17] or experimental studies alone [13]. The following research proposes an analytical framework to overcome the shortcomings of experimental studies and numerical simulation approaches.

III. Master Equation Approach

Real-life traffic flows in the near future will typically include ACC-enabled and human-driven vehicles. One would not wish to discover, after such mixed vehicle environments emerge, that the interaction between human and automated driver behavior induces or magnifies congestion effects. The fact that ACC-enabled and human-driven vehicles will most probably be randomly distributed in the traffic stream necessitates a probabilistic approach for analyzing the impact of ACC penetration on traffic flow. The master equation, which describes the time evolution of the probability distribution of system states, is a helpful tool for performing such an analysis. The master equation approach for analyzing the dynamics of the size a vehicle cluster (or traffic jam) is described in the following subsections.

A. Vehicle Cluster (or Traffic Jam) Dynamics

To simplify the study of highway traffic, the system is often idealized as a single lane road forming a closed ring of length L with N vehicles on it [23], [24] as shown in Fig. 1. The primary reason in support of this idealization is that it helps avoid dealing with an open system representation of a highway which may include on- and off-ramps. The presence of ramps would require additional boundary conditions and could potentially complicate the system analysis. When the closed-road system is observed at the microscopic level, each vehicle in the traffic flow can be in one of two states: (i) the vehicle is in free flow, i.e. it moves independently of any other vehicles on the road, and (ii) the vehicle is stuck in a cluster or traffic jam. A consequence of this definition of the state is that at the microscopic level, the total number of possible states is 2^N. However, when studying the system at a mesoscopic scale, the state of choice is the cluster size (n), or the aggregate number of vehicles stuck in a cluster at time t, and the total number of states is N.

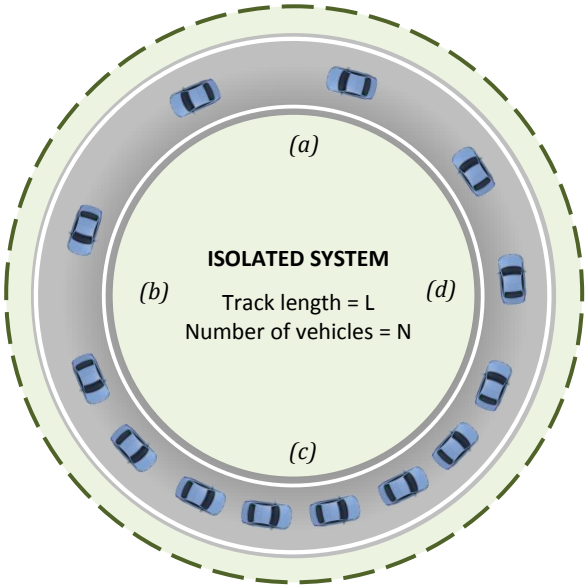

Fig. 1. Single lane closed road system under consideration. (a) Vehicles in free flow, (b) Vehicles transitioning from free flow to jammed state (joining a cluster), (c) Vehicles stuck inside a traffic jam (cluster), and (d) Vehicles transitioning from jammed state to free flow state.

Mahnke and Pieret [5] model the formation of clusters, or

self-organized traffic jams, using the mesoscopic definition of the system state. Specifically, the dynamics of the system in [5] are modeled as a stochastic process in terms of the probability distribution of the states, using a master equation as follows:

$$\frac{d}{dt}P(n,t) = \sum_{n' \neq n} [w(n',n)P(n',t) - w(n,n')P(n,t)] \quad (1)$$

where, $w(n',n)$ denotes the transition probability rate of going from state n' to state n, i.e. the cluster size changes from n' to n, $P(n',t)$ denotes the probability that n' vehicles are stuck in a cluster at time t, $w(n,n')$ denotes the transition probability rate of going from state n to n', and $P(n,t)$ denotes the probability that n vehicles are stuck in a cluster at time t. Under the assumption that only one vehicle may join or leave the traffic jam at any time instant t, i.e. the state n can only transition to neighboring states ($n-1$, n or $n+1$), the master equation reduces to:

$$\begin{aligned}\frac{d}{dt}P(n,t) = {} & w(n-1,n)P(n-1,t) \\ & + w(n+1,n)P(n+1,t) \\ & - \{w(n,n+1) + w(n,n-1)\}P(n,t)\end{aligned} \quad (2)$$

Mahnke and Pieret [5] further develop the master equation approach to study the dynamics of the expected cluster size $\langle n \rangle = \sum_n nP(n,t)$. Through simple algebraic operations on (2), the following equation for the dynamics of the expected cluster size $\langle n \rangle$ is obtained:

$$\begin{aligned}&\frac{d}{dt}\langle n \rangle = \frac{d}{dt}\sum_n nP(n,t) = \\ &\sum_n n\begin{Bmatrix} w_+(n-1)P(n-1,t) + w_-(n+1)P(n+1,t) \\ -[w_+(n) + w_-(n)]P(n,t) \end{Bmatrix}\end{aligned} \quad (3)$$

where $w_+(n)$ denotes the transition probability rate of a vehicle joining a cluster of size n from free flow and creating a cluster of size $(n+1)$, $w_-(n)$ denotes the transition probability rate of a vehicle leaving a cluster of size n and creating a cluster of size $(n-1)$, and $\langle \cdot \rangle$ denotes the expectation operator. Further expanding the expression under the summation sign in (3) and using the boundary conditions:

$$\begin{aligned}\frac{d}{dt}P(0,t) &= w_-(1)P(1,t) - w_+(0)P(0,t) \\ \frac{d}{dt}P(N,t) &= w_+(N-1)P(N-1,t) - w_-(N)P(N,t)\end{aligned} \quad (4)$$

the dynamics of the expected cluster size are obtained to be:

$$\frac{d}{dt}\langle n \rangle = \langle w_+(n) \rangle - \langle w_-(n) \rangle \quad (5)$$

The mean field approximation is used to approximate the expected value of the transition probability rates at a given cluster size n ($\langle w(n) \rangle$), with the transition probability rates of the expected value of the cluster size (w$\langle n \rangle$). Thus, the dynamics of the expected vehicle cluster size are as follows:

$$\frac{d}{dt}\langle n \rangle = w_+\langle n \rangle - w_-\langle n \rangle \quad (6)$$

B. Transition Probability Rates

In order to completely describe the vehicle cluster dynamics, it is necessary to know the functional form of the transition probability rates in (6). The transition probability rate $w_+(n)$ of a vehicle joining a cluster of size n is defined as the inverse of the time taken for a vehicle in free flow to join a cluster. Further, the time taken for a vehicle to join a cluster (t_{join}) is dependent on the car-following or cruise control algorithm employed, as well as the initial headway in free flow. Since typical vehicle headways in a traffic jam are of the order of 1-2 m, a following vehicle is said to have 'joined' a cluster when it attains this headway [5]. Similarly, the transition probability rate $w_-(n)$ of a vehicle leaving a cluster of size n is defined as the inverse of the time taken to accelerate out of a cluster into free flow traffic. Further, this time taken for a vehicle to leave a cluster (t_{leave}) is determined using a simple constant acceleration model as described in [26] [27], and is assumed to be constant for both ACC-enabled and human-driven vehicles.

Mahnke and Pieret present an expression for $w_+\langle n \rangle$ by assuming that vehicles join the cluster by moving at a constant speed and 'colliding' with the cluster, irrespective of the driver's efforts to maintain a safe velocity and distance from the preceding vehicle during the 'collision' process [22]. This simple approximation, while a good first step towards modeling self-organizing traffic jams, does not reflect the true driver behavior while approaching a cluster. Instead, in this study, new transition probability rates are determined based on car-following or ACC algorithms to more accurately describe driver behavior.

IV. New Transition Probability Rates

In the present study, new transition rates are derived based on car-following models to accurately represent driver behavior. While the presented analysis uses a specific car-following algorithm, in general any algorithm for which analytical expressions for $w_+(n)$ and $w_-(n)$ can be calculated may be used. Though the number of such car-following algorithms is probably limited in number, the analytical procedure presented here does provide deeper insight into the effects of ACC penetration on formation of self-organized traffic jams. Consequently, it is a potentially useful tool for studying changes in traffic jam dynamics with increasing ACC penetration and designing improvised ACC algorithms. The following subsections discuss the car-following algorithm employed, the procedure for calculating the new transition probability rates, and the associated assumptions.

A. General Motors' Car-following Model

One of the popular, validated and intuitively simple car-following algorithms is the General Motors' (GM) fourth model proposed by the General Motors Research Group

around 1960 [6] [28]. The model determines the acceleration control effort to be applied to the vehicle by using three variables: the headway to the preceding vehicle, the relative velocity between the vehicle under consideration and the preceding vehicle, and the absolute velocity of the vehicle under consideration. Specifically,

$$\ddot{x}_{n+1}(t+\Delta t) = \frac{\alpha\,[\dot{x}_{n+1}(t+\Delta t)]}{[x_n(t) - x_{n+1}(t)]}\left(\dot{x}_n(t) - \dot{x}_{n+1}(t)\right) \quad (7)$$

where $x_{n+1}(t)$ denotes the position of the vehicle entering the cluster, $x_n(t)$ denotes the position of the preceding vehicle (or the vehicle at the tail-end in the cluster), α denotes the sensitivity of the driver of the vehicle entering the cluster, and Δt denotes the reaction time. For sake of brevity, the headway $x_n(t) - x_{n+1}(t)$ is represented by $h(t)$ in the remainder of this paper. Fig. 2 depicts the different variables that will be used in the development of the analytical framework.

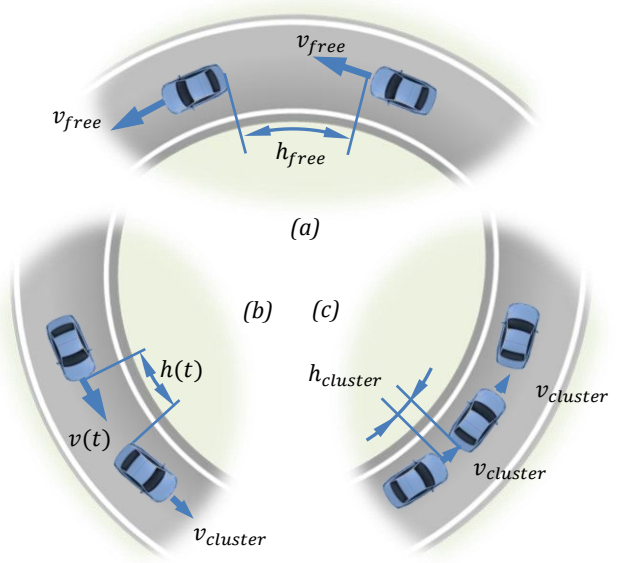

Fig. 2. Description of variables used in analysis. (a) Vehicles in free flow: h_{free} = Free flow headway, v_{free} = Free flow velocity; (b) Vehicles transitioning from free flow to jammed state (joining a cluster): $h(t)$ = Headway as a function of time, $v(t)$ = Velocity as a function of time; (c) Vehicles stuck inside a traffic jam (cluster): $h_{cluster}$ = Headway inside a cluster, $v_{cluster}$ = Velocity inside a cluster.

The driver sensitivity (α) is typically indicative of the alertness of the driver while following a preceding vehicle. Low driver sensitivity might represent a 'sleepy' driver who takes longer to react to maneuvers, such as braking, performed by the preceding vehicle. On the other hand, high driver sensitivity might represent an 'alert' driver, who is cognizant of any maneuvers performed by the preceding vehicle and tends to take any necessary action well in advance.

When considering the scenario of a vehicle entering a cluster, the range of admissible driver sensitivities is determined using typical traffic conditions and comfortable deceleration standards set by the American Association of State Highway and Transportation Officials (AASHTO). The typical traffic flow is assumed to have free flow velocity of about 25 m/s (about 55 miles/hour), free flow headway of about 100 m, and cluster velocity of about 0-2 m/s. Further, the maximum permissible deceleration is limited to 3.4 m/s^2, according to AASHTO standards. The admissible driver sensitivities that may be used with the GM fourth model under such constraints are determined by simulating the process of entering a cluster for vehicles with varying driver sensitivities. Fig. 3 depicts the acceleration profile for a vehicle entering a cluster while using the GM fourth model as the ACC algorithm. The acceleration profiles suggest that the algorithms with low driver sensitivity react much later than algorithms with high driver sensitivity. Only those driver sensitivities for which maximum deceleration during the process of entering the cluster is within the range of values suggested by the AASHTO roadway usage standard are considered for further analysis. The simulations were repeated for different values of driver sensitivity and the maximum deceleration observed during each simulation was recorded.

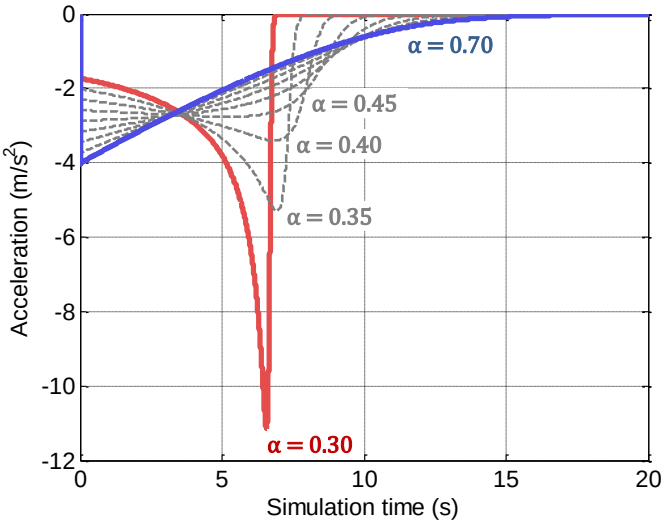

Fig. 3. Acceleration vs. time profile for vehicle entering a cluster with ACC algorithm based on GM fourth model. A driver model with low driver sensitivity ($\alpha = 0.3$) reacts later than a driver with high driver sensitivity ($\alpha = 0.7$).

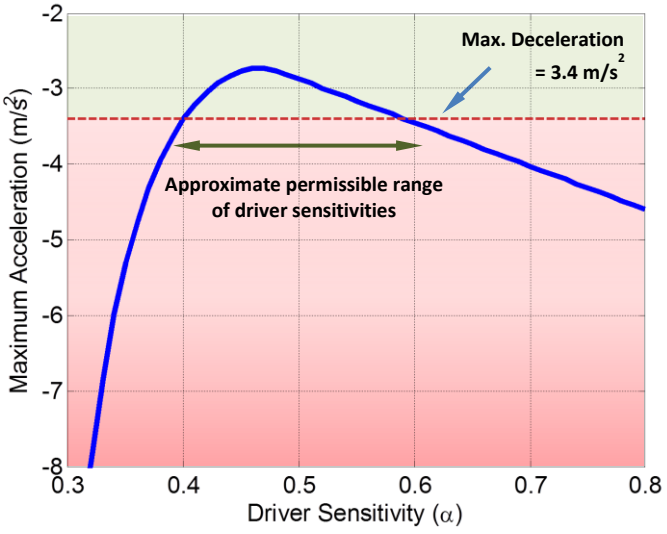

Fig. 4. Maximum observed deceleration during simulation of a vehicle joining a cluster in typical traffic conditions, with varying driver sensitivities. The range of admissible driver sensitivities is approximately [0.4, 0.6].

Fig. 4 shows the maximum deceleration observed during the process of entering a cluster for vehicles with various driver sensitivities. Driver sensitivities that lie approximately in the range [0.4, 0.6] are admissible values for use in the GM fourth model. With this insight, the GM car-following model can now be used to determine the transition probability rates associated with it.

B. Derivation of New Transition Probability Rates

Section III discussed that the transition probability rate for a vehicle joining a cluster may be defined as the inverse of the time taken to join a cluster. Since all parameters relevant to the GM fourth car-following model have been specified, the nonlinear ODE describing the applied acceleration effort (7) can now be solved for the time taken for a vehicle to join a cluster, using the initial and boundary conditions specified by typical traffic flow conditions. Rewriting (7) in terms of the headway $h(t) = x_n(t) - x_{n+1}(t)$, and neglecting the reaction time Δt, we get:

$$h\ddot{h} = \alpha(\dot{h} - v_c)\dot{h} \tag{8}$$

where v_c denotes the velocity of the preceding vehicle. In the specific case of a vehicle entering a traffic jam, the preceding vehicle is the one at the tail-end of a vehicle cluster and its velocity v_c is assumed to be constant. Equation (8) may be re-written as follows:

$$\frac{\ddot{h}}{\dot{h}} = \frac{\alpha(\dot{h} - v_c)}{h} \tag{9}$$

which after some simplification results in:

$$\frac{d}{dh}(\dot{h}) = \frac{\alpha(\dot{h} - v_c)}{h} \tag{10}$$

or,

$$\frac{d\dot{h}}{(\dot{h} - v_c)} = \alpha\frac{dh}{h} \tag{11}$$

Integration of both sides of (11) yields:

$$\ln(\dot{h} - v_c) = \alpha\ln(h) + \ln(c) \tag{12}$$

or,

$$\dot{h} - v_c = ch^\alpha \tag{13}$$

Using boundary conditions corresponding to typical free flow traffic, the constant c is calculated to be $c = -k = -v_{free}/h_{free}^\alpha$. Substituting the value of c back into (13) and rearranging the terms, we get:

$$dt = \frac{dh}{v_c - kh^\alpha} \tag{14}$$

In order to determine the transition probability rate ($w_+(n)$) of joining a traffic jam with n vehicles in it, the time taken to join a vehicle cluster from free flow needs to be derived. The derivation for time taken to reach the tail end of an existing vehicle cluster, starting from free flow headway, is included below. Integrating both sides of (14), we get:

$$\int_0^t dt = \int_{h_{free}}^{h} \frac{h_{free}^\alpha}{v_c h_{free}^\alpha - v_{free}h^\alpha}dh \tag{15}$$

or,

$$t = \frac{1}{v_c}\int_{h_{free}}^{h} 1 + \frac{v_{free}h^\alpha}{v_c h_{free}^\alpha - v_{free}h^\alpha}dh \tag{16}$$

or,

$$t = \frac{h - h_{free}}{v_c} - \frac{1}{v_c}\int_{h_{free}}^{h} \frac{1}{1 - \frac{v_c h_{free}^\alpha}{v_{free}h^\alpha}}\,dh \tag{17}$$

Now, realizing that as the vehicle approaches a traffic jam, its headway decreases with time, i.e. $\dot{h} < 0$, we can deduce the following from (13):

$$\dot{h} = v_c - \frac{v_{free}h^\alpha}{h_{free}^\alpha} < 0 \tag{18}$$

or,

$$\frac{v_c h_{free}^\alpha}{v_{free}h^\alpha} < 1 \tag{19}$$

Using the Maclaurin series for the expansion of $(1-x)^{-1}$ for $x < 1$, the expression in (17) is operated upon to get:

$$t = \frac{h - h_{free}}{v_c} - \int_{h_{free}}^{h} \frac{1}{v_c}\left\{1 + \left(\frac{v_c h_{free}^\alpha}{v_{free}h^\alpha}\right) + \left(\frac{v_c h_{free}^\alpha}{v_{free}h^\alpha}\right)^2 + \cdots\right\}dh \tag{20}$$

or,

$$t = \frac{h - h_{free}}{v_c} - \frac{1}{v_c}\left\{1 + \left(\frac{v_c h_{free}^\alpha}{v_{free}}\right)\frac{h^{1-\alpha}}{1-\alpha} + \left(\frac{v_c h_{free}^\alpha}{v_{free}}\right)^2\frac{h^{1-2\alpha}}{1-2\alpha} + \cdots\right\}_{h=h_{free}}^{h=h} \tag{21}$$

Equation (21) holds true for all $\alpha \neq 1/m$. However, in case $\alpha = 1/m$, the integral of the corresponding m^{th} term can be modified accordingly to yield an expression in terms of $ln(h)$. Simplifying (21) and using the limits of integration corresponding to headway in free flow traffic (h_{free}) and headway inside a vehicle cluster (h_c), the following expression is obtained:

$$t_{join} = \frac{1}{v_c}\sum_{m=1}^{\infty}\left\{\frac{1}{1-m\alpha}\left(\frac{v_c}{k}\right)^m\left(h_{free}^{1-m\alpha} - h_c^{1-m\alpha}\right)\right\} \tag{22}$$

where t_{join} denotes the time taken to join a cluster, v_c denotes the velocity of the vehicle at the tail-end in the cluster (also the preceding vehicle for the vehicle joining the cluster), m refers to the m^{th} term in the series expansion, α denotes the driver sensitivity in the GM fourth car following model, $k = v_{free}/h_{free}^\alpha$ denotes a driver dependent constant, and h_c denotes the headway inside a cluster and is known to be

approximately constant at about 1 meter through experimental observations [5] [22].

Unfortunately, the expression for t_{join} is a hypergeometric series with no closed-form solution. However, it is observed that as an increasing number of terms are used in calculating t_{join}, i.e. the series is truncated at higher orders of m, the hypergeometric series quickly converges to the true solution obtained from numerical simulation. Fig. 5 depicts the convergence of the hypergeometric series to the exact solution. As can be observed, the approximate solution is comparable to the exact solution for even as few as two terms.

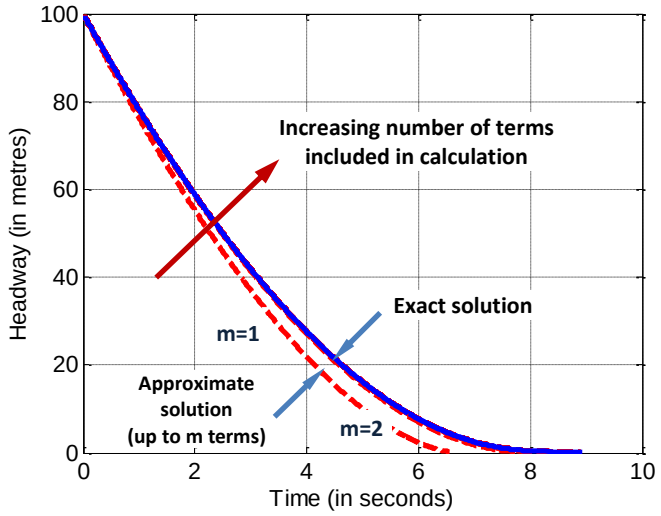

Fig. 5. Time taken to join a cluster (t_{join}) using expression derived from GM fourth model nonlinear ODE. The truncated hypergeometric series quickly converges to the exact solution as more terms are added.

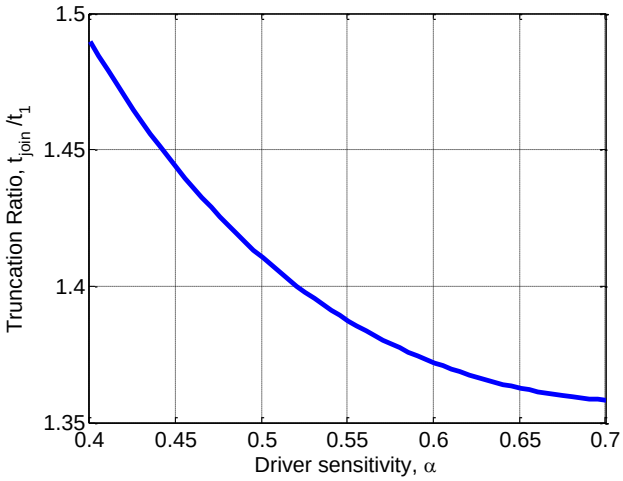

Fig. 6. Range of admissible driver sensitivities limits the variation of truncation ratio, $T_R = t_{join}/t_1$. Based on the driver sensitivity α of the car-following algorithm, an appropriate value of T_R can be used to approximate the time taken to join a cluster.

An additional key insight of this paper is to recognize that the hypergeometric series is constrained by the range of admissible driver sensitivities. Considering the range of admissible driver sensitivities, it is observed that a closed-form exact solution of the hypergeometric series t_{join} can be approximated by using the first term of the series (t_1) and an appropriate truncation ratio (T_R), such that $t_{join} = T_R t_1$. Fig. 6 depicts the variation in the truncation ratio, which is the ratio of the exact solution obtained from numerical solution and the approximate solution obtained using only the first term of the series, as a function of driver sensitivity α. Thus, when the driver sensitivity of the car following algorithm is known, Fig. 6 may be used to determine the correct truncation ratio and, consequently, the approximate time (t_{join}) taken to join the vehicle cluster.

As mentioned earlier, the transition probability rate is defined as the inverse of the time taken to join a cluster. Thus, the new transition probability rate for a vehicle joining a cluster is given by:

$$w_+(n) = \frac{1}{t_{join}} = \frac{1}{T_R\, t_1} = \frac{k(1-\alpha)}{T_R}\left(\frac{1}{h_{free}^{1-\alpha} - h_c^{1-\alpha}}\right) \qquad (23)$$

The transition probability rate for leaving a cluster is determined using a constant acceleration model and is assumed to be constant for both ACC-enabled and human-driven vehicles. The acceleration of a vehicle starting out of a cluster and moving into free flow is determined by modeling it as a vehicle starting from rest. From experimental observations [27] of traffic, this acceleration is found to be 2.5 m/s^2 on an average and the corresponding time taken to leave the cluster based on typical traffic conditions is 7.5-10 seconds. As a result, $w_-\langle n\rangle = 1/t_{leave}$ is approximately equal to 0.1s^{-1}. Thus, new transition probability rates that better describe actual driver behavior have been obtained and further analysis based on the vehicle cluster dynamics as described by (6) can be performed.

V. Steady-State Analysis

The vehicle cluster dynamics discussed in the Section III may be used to perform a steady-state analysis to determine the expected size of a stable cluster or traffic jam. This section will discuss how the expected cluster size varies as a function of traffic density in steady-state conditions, for both single species and multi-species environments.

A. Steady-state Analysis for Single Species Environment

As is evident from (6), the steady-state condition for a stable cluster size is $w_+\langle n\rangle = w_-\langle n\rangle$. Since $w_+\langle n\rangle$ is a function of the free flow headway (h_{free}), as derived from the GM fourth model and described in (23), and $w_-\langle n\rangle$ has been assumed to be constant, the steady-state condition can be used to determine an expression of h_{free} as follows:

$$\left[h_{free}\right]_{ss} = \left\{h_c^{1-\alpha} + \frac{t_{leave}k(1-\alpha)}{T_R}\right\}^{1/1-\alpha} \qquad (24)$$

Additionally, physical constraints such as the finite length of the closed road and finite vehicle length can also be used to determine the free headway. These two expressions for free flow headway, one obtained from the steady-state condition and the other from physical constraints, can then be equated as follows:

$$\left[h_{free}\right]_{ss} = \frac{L - Nl - (\langle n\rangle - 1)h_c}{N - \langle n\rangle + 1} \tag{25}$$

where l denotes the length of a vehicle. Further, assuming that the expected cluster size is large, so that $\langle n\rangle - 1 \approx \langle n\rangle$, dividing the numerator and denominator on the right hand side by L, and with some rearrangement, the following expression that relates the expected cluster size to the traffic density is obtained:

$$\langle n\rangle^* = \frac{\rho^*\left(\left[h_{free}\right]_{ss} + l\right) - l}{\left(\left[h_{free}\right]_{ss} - h_c\right)} \tag{26}$$

where $\langle n\rangle^* = \langle n\rangle l/L$ denotes the normalized expected cluster size, and $\rho^* = Nl/L$ denotes the dimensionless traffic density on the closed road. Equation (26) indicates that the relationship between stable cluster size and traffic density is linear in nature. Further, since the cluster size cannot be less than zero, (26) also indicates that there exists a critical density ρ_c at which vehicle clusters or self-organized traffic jams first begin to appear. Substituting $\langle n\rangle^* = 0$ in (26) yields an expression for dimensionless critical density for a traffic flow:

$$\rho_c^* = \frac{l}{\left[h_{free}\right]_{ss} + l} \tag{27}$$

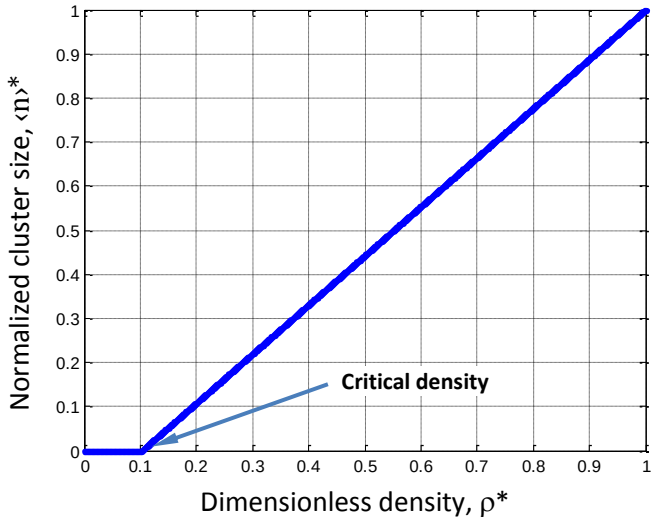

Fig. 7. Steady-state phase portrait of normalized cluster size versus dimensionless density consisting of singe driver species based on GM fourth model with $\alpha = 0.4$. The solid line indicates stable cluster sizes or traffic jams. Clusters or traffic jams first begin to appear when the dimensionless density reaches a critical value of $\rho_c^* = 0.1$.

Fig. 7 shows the steady-state phase plot of the normalized stable cluster size plotted against the dimensionless density for a traffic flow consisting of a single species, or a single type of driver model (GM fourth model) with driver sensitivity $\alpha = 0.4$. The solid line depicts the stable cluster size for a given density. It is observed that in this scenario, the analytical results predict that the dimensionless critical density, or the density at which vehicle clusters begin to form spontaneously, is $\rho_c^* = 0.1$. It is argued that the value of the driver sensitivity, $\alpha = 0.4$, is reasonably representative of human drivers since experimental data from German highways (shown in Fig. 8) also indicates that the dimensionless critical density for humans, as observed from the fundamental diagram of traffic flow, is approximately 0.1. In the next subsection we discuss the selection of the appropriate driver sensitivity for ACC-enabled vehicles and the methodology for introducing ACC-enabled vehicles in the analysis framework.

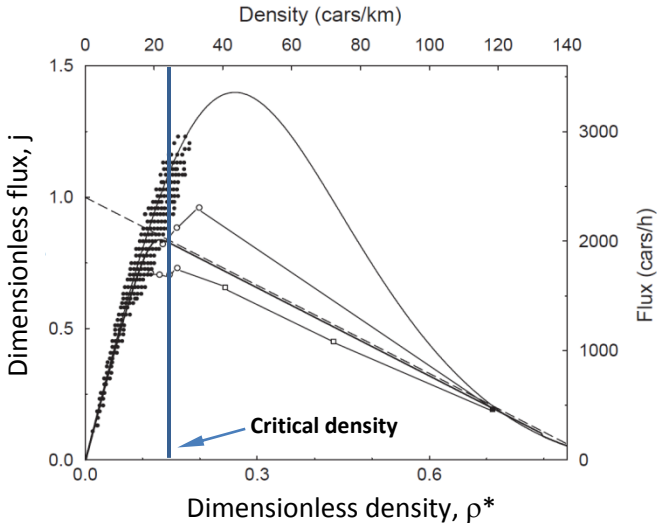

Fig. 8. Experimental data for traffic flow consisting solely of human drivers on German highways. Dots indicate experimental observations [29]. The observed dimensionless critical density is close to 0.1 [23].

B. *Introduction of ACC-enabled Vehicles into Traffic Flow*

The single-lane closed ring system is now considered with traffic consisting of a mixture of ACC-enabled and human-driven vehicles. Let the proportion of ACC-enabled vehicles on the closed road be p. Assuming that the population of vehicles on the closed road is large enough, such that the proportion of ACC-enabled and human-driven vehicles outside the cluster remains constant, then the effective transition probability rates are given by:

$$\begin{aligned} w_+^{eff}(n) &= (1-p)w_+^H(n) + pw_+^{ACC}(n); \\ w_-^{eff}(n) &= 1/t_{leave} \end{aligned} \tag{28}$$

where $w_+^H(n)$ denotes transition probability rate of joining a cluster for a human-driven vehicle with $\alpha_H = 0.4$, and $w_+^{ACC}(n)$ denotes transition probability rate of joining a cluster for an ACC-enabled vehicle with $\alpha_{ACC} = 0.7$. The rationale behind picking the driver sensitivity value for human drivers has already been presented in the previous subsection.

In contrast, the choice of driver sensitivity for ACC-enabled vehicles is motivated in part by the reasoning that, whereas human drivers are typically performing multiple tasks while driving and may be less alert to sudden changes in the traffic stream ahead, ACC algorithms are performing the sole task of driving and continually monitoring the road ahead. ACC algorithms are expected to be more sensitive and alert to changes in the traffic stream and thus are assigned a higher driver sensitivity value. Another motivating factor for choosing $\alpha_{ACC} = 0.7$ is the desire to obtain a closed-form

solution for the expected vehicle cluster size. This is discussed in the next subsection in relation with the steady-state analysis for mixed traffic.

C. Steady-state Analysis for Multi-species Environment

The sensitivity value for ACC-enabled vehicles is determined from the necessity of obtaining a closed form solution for the analysis. When the expressions for individual transitional probabilities $w_+^H(n)$ and $w_+^{ACC}(n)$ are substituted in the effective transition probability rate $w_+^{eff}(n)$ and the steady-state condition $w_+^{eff}\langle n\rangle = w_-^{eff}\langle n\rangle$ is considered, the following equation is obtained:

$$h_{free}^{1-\alpha_H} h_{free}^{1-\alpha_{ACC}} - b h_{free}^{1-\alpha_H} - c h_{free}^{1-\alpha_{ACC}} + d = 0 \qquad (29)$$

where b, c, and d are functions of h_c, t_{leave}, p, α_{ACC}, and α_H, and are given by:

$b = h_c^{1-\alpha_{ACC}} + (1-\alpha_{ACC}) p t_{leave} k_H / T_{R,ACC}$,

$c = h_c^{1-\alpha_H} + (1-\alpha_H)(1-p) t_{leave} k_{ACC} / T_{R,H}$, and

$d = h_c^{1-\alpha_H} h_c^{1-\alpha_{ACC}} + (1-\alpha_H)(1-p) t_{leave} k_H h_c^{1-\alpha_{ACC}} / T_{R,H} + p(1-\alpha_{ACC}) t_{leave} k_{ACC} h_c^{1-\alpha_H} / T_{R,ACC}$

where T_R and k are functions of driver sensitivity α, as discussed earlier.

In the depicted general form, (29) is a transcendental equation and can only be solved using numerical or graphical methods. In order to obtain an analytical solution for the steady-state free headway, the transcendental equation is reduced to an algebraic equation (quadratic, cubic or bi-quadratic) by enforcing a constraining relation on the values that α_H and α_{ACC} may simultaneously assume. One such relation that reduces equation (29) into a cubic equation and thus allows a closed-form solution is $(1-\alpha_H) = 2(1-\alpha_{ACC})$, i.e. $\alpha_{ACC} = 0.5(1+\alpha_H)$. It may be observed that, once this substitution is made, arbitrary choices of driver sensitivities cannot be made in further analysis. This is due to the fact that the choices are restricted by two constraints, viz. the maximum acceptable deceleration, and a constraining relation between α_{ACC} and α_H which is a consequence of the need to obtain a closed form solution. A number of values of driver sensitivities (α_H, α_{ACC}) such as (0.35, 0.675), (0.4, 0.7) etc. which satisfy the relation $(1-\alpha_H) = 2(1-\alpha_{ACC})$ also lie approximately in the range defined by maximum acceptable deceleration based on AASHTO standards.

Thus, the relation $(1-\alpha_H) = 2(1-\alpha_{ACC})$ may be used as an approximation, together with this restricted set of values, to reduce equation (29) into a cubic form as follows:

$$\left(h_{free}^{1-\alpha_{ACC}}\right)^3 - b\left(h_{free}^{1-\alpha_{ACC}}\right)^2 - c\left(h_{free}^{1-\alpha_{ACC}}\right) + d = 0 \qquad (30)$$

The expression for steady-state free headway $\left[h_{free}\right]_{ss}$ in a multi-species environment is obtained by solving the cubic equation (30). Next, the steady-state free headway expression is substituted into (26) to obtain a relationship between expected cluster size and traffic density in a multi-species environment. The implications of the above analysis in both single species and multi-species traffic environments are discussed in the next section, along with experimental results from mesoscopic simulations of the traffic flow.

VI. Results and Mesoscopic Simulations

This section discusses the obtained analytical results for both single species and multi-species environments, and their interpretations with respect to real-life traffic flows. Additionally, mesoscopic simulations of vehicle cluster dynamics are presented and are shown to validate the obtained analytical results.

A. Results for Single Species Traffic Flow

In the previous section it was mentioned that the expression for steady-state free headway obtained from (30) may be substituted in (26) to obtain the relationship between expected normalized cluster size and dimensionless density in a multi-species environment. The resulting relationship may be plotted as a phase portrait to illustrate the cluster dynamics as a function of the proportion of ACC-enabled vehicles on the closed road. Fig. 9 shows the steady-state phase portraits for two special cases: (i) when the vehicle population consists of only human-driven vehicles $(p = 0, \alpha = 0.4)$, and (ii) when the vehicle population consists of only ACC-enabled vehicles $(p = 1, \alpha = 0.7)$. The figure suggests that the traffic operates at *higher* critical densities, and consequently *higher* traffic flows, when it consists of only ACC-enabled vehicles as compared to when it consists of only human-driven vehicles. The relationship between cluster size and density in a single-species environment is validated by performing a Monte Carlo simulation using the mesoscopic level definition and dynamics of the system state. Specifically, the cluster formation process is modeled as a one-dimensional random walk where the cluster size grows or shrinks based on the new transition probabilities derived in Section IV.

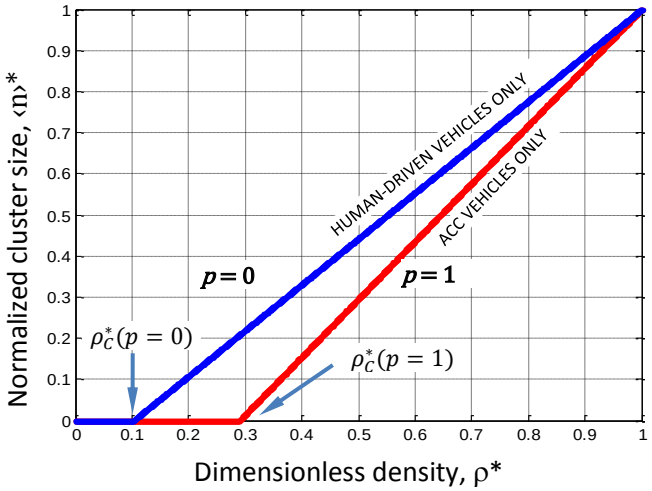

Fig. 9. Steady-state phase portrait for special cases of mixed traffic analytical results. Traffic consists of: (i) human-driven vehicles alone (p=0), and (ii) ACC vehicles alone (p=1).

Fig. 10 shows that the mesoscopic simulation matches the analytical results but is valid only up to dimensionless density $\rho^* = 0.8$. This can be explained by studying the

method for calculating free headway from physical constraints, as described in (25). It is evident that as $N \to L/l$, the numerator on the right-hand side of (25) becomes smaller, and represents the limit of bumper-to-bumper traffic. Any further subtraction due to the presence of the cluster headway term, $(\langle n \rangle - 1)h_{cluster}$, will cause the free headway to become negative. Thus, the simulation indicates that present form of the analysis may not be applicable for extremely high density traffic. However, it may be realized that situations in which the traffic flow reaches extremely high densities are not expected to be observed too often. The analysis is largely supported by the simulations in the remaining scenarios, especially for determining the critical density at which vehicle clusters (or traffic jams) first appear.

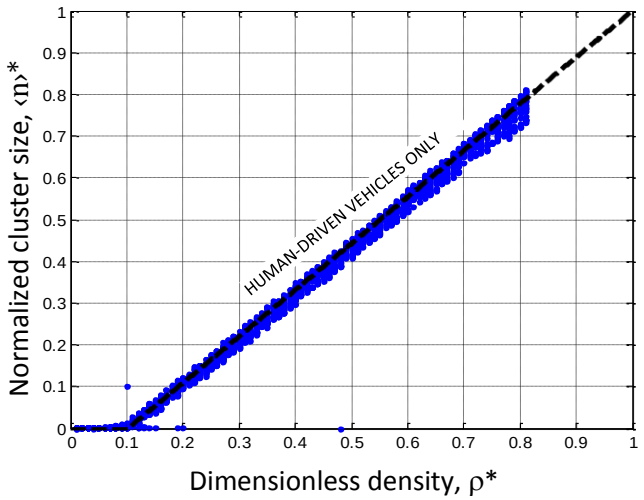

Fig. 10. Monte Carlo simulation validates the analytical results obtained for the relationship between normalized cluster size and dimensionless density, for a single species environment. Thick dashed line denotes analytical solution. Solid dots indicate the mean steady-state cluster sizes obtained from the simulation.

B. Results for Multi-species or Mixed Traffic Flow

In a multi-species environment, it is of greater interest to observe the trends in critical density as a function of the proportion of ACC-enabled vehicles in the mixed traffic flow. Fig. 11 shows these trends as obtained from the analytical results. It is observed that as the proportion of ACC-enabled vehicles on the road is increased, the critical density increases and this increase is not uniform. Specifically, as the proportion of ACC-enabled vehicles in the traffic flow increases, the traffic flow becomes increasingly sensitive to changes in vehicle population proportions. For example, consider the two scenarios in Fig. 11 that depict the traffic system operating at the same threshold ($\Delta\rho$) away from the critical density, but in two very different regimes. In predominantly human driver traffic in the jam-free regime (operating point A), a small change in vehicle proportion (Δp) does not change the state of the traffic flow, which continues to operate in the jam-free regime. On the other hand, if the same change of vehicle proportion is introduced in predominantly ACC traffic in the jam-free regime (operating point B), it causes the traffic flow to change from a jam-free state to a self-organized jam or congested state. The same trend can be observed by studying the sensitivity of critical density to proportion of ACC-enabled vehicles, which is defined as follows:

$$Sensitivity, s(p_0) = \left(\frac{d\rho_C^*}{dp}\right)_{p=p_0} \quad (31)$$

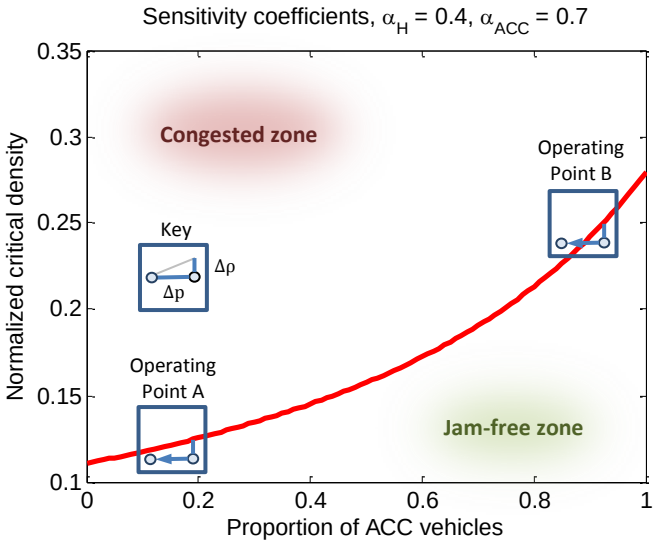

Fig. 11. Increased ACC penetration results in an increase in the critical density at which traffic jams first appear. Points A and B operate at the same threshold (Δρ) away from the critical density line. Identical changes in vehicle proportion (Δp) produce different results at the operating points.

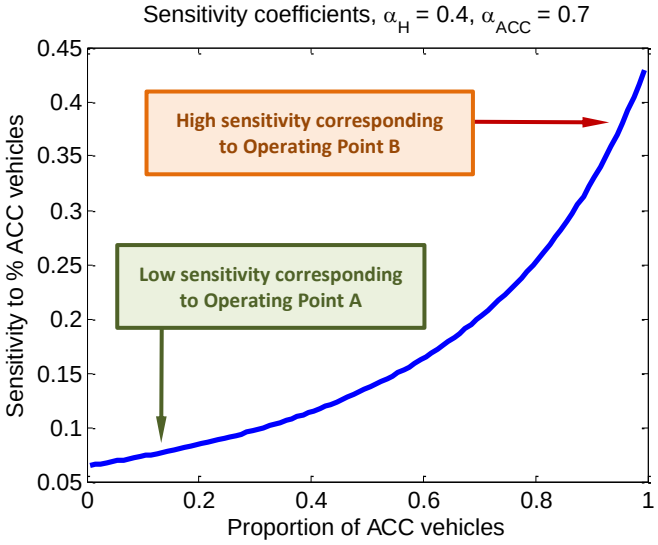

Fig. 12. Sensitivity of critical density to ACC penetration. Traffic flows with high ACC penetration are up to 10 times more susceptible to formation of self-organized traffic jams, as compared to traffic flows with low ACC penetration.

Fig. 12 indicates that for roadways operating at or near peak flow capacity, traffic systems with very high ACC penetration are up to 10 times more susceptible to congestion caused by self-organized traffic jams as compared to traffic systems with very low ACC penetration. In other words, in medium-to-high density traffic, the introduction of a small percentage of human-driven vehicles into a predominantly ACC-enabled vehicle population is more likely to cause a "phantom" traffic jam as compared to the introduction of the same percentage of

human-driven vehicles in an already predominantly human-driven vehicle population.

In the previous subsection, it was shown that the analytical results for critical density are well supported by the mesoscopic simulations. Extending the analysis to multi-species systems, Monte Carlo simulations are used to determine the normalized critical density as the proportion of ACC-enabled vehicles on the road increases. Fig. 13 shows the Monte Carlo simulation results with 1000 iterations and varying percentage of ACC-enabled vehicles in the traffic stream. The isolines on the contour map indicate the number of iterations (out of a total 1000 iterations) in which a vehicular cluster was observed. The simulations indicate that the lower bound of the contour map appears to agree very well with the analytical result for normalized critical density, which is depicted using the dashed line in Fig. 13.

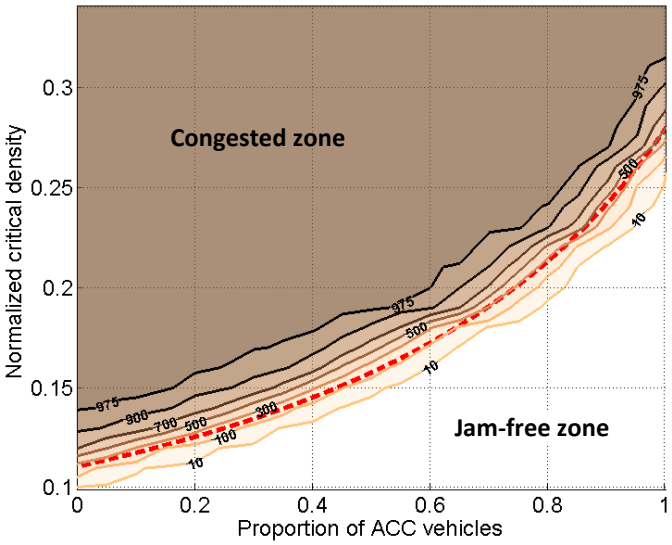

Fig. 13. Results from the Monte Carlo simulation for mixed traffic flow appear to agree with the analytical results. Isolines indicate number of simulations (out of 1000 total iterations) that resulted in a vehicular cluster (self-organized traffic jam). Dashed line indicates normalized critical density obtained from analytical results.

VII. Conclusions

The present study has developed analytical results to determine the impact of the introduction of ACC-enabled vehicles on traffic flow and congestion. It has been shown that as the percentage of ACC-enabled vehicles in the traffic stream is increased the critical density also increases correspondingly. In other words, as more ACC-enabled vehicles join the traffic stream, the density at which vehicle clusters begin to spontaneously appear increases. This indicates that the traffic flow can operate at higher densities and consequently higher flow rates.

Additionally, the study also found that while increased ACC penetration may allow the traffic system to operate at increased densities and flows, it comes at a cost. As ACC penetration increases, a small increase in the percentage of human drivers may be enough to cause congestion. In other words, in a predominantly ACC traffic system, introduction of human-driven vehicles may cause a rapid reduction of critical density, resulting in a self-organized traffic jam. The knowledge gleaned from the analysis presented in this paper may be used to improve upon and design better ACC algorithms that take into account the functional relationship between ACC penetration and traffic jam dynamics. This knowledge could mitigate the environmental, financial and productivity losses arising due to self-organized traffic jams.

References

[1] FHWA, "Our nation's highways 2008," US DoT, Washington D.C., 2008.

[2] D. L. Shrank and T. J. Tomax, "The 2007 Urban Mobility Report," Texas Transportation Institute, 2007.

[3] B. S. Kerner and P. Konhauser, "Cluster effect in initially homogeneous traffic flow," *Physical Review E*, vol. 48, no. 4, pp. 2335-2338, 1993.

[4] Y. Sugiyama, M. Fukui, M. Kikuchi, K. Hasebe, A. Nakayama, K. Nishinari, S. Tadaki and S. Yukawa, "Traffic jams without bottlenecks - experimental evidence for the physical mechanism of the formation of a jam," *New Journal of Physics*, vol. 10, 2008.

[5] R. Mahnke and N. Pieret, "Stochastic master-equation approach to aggregation in freeway traffic," *Physical Review E*, vol. 56, no. 3, pp. 2666-2671, 1997.

[6] D. C. Gazis, H. R and P. R. B, "Car-following Theory of Steady-state Traffic Flow," *Operations Research*, vol. 7, no. 4, pp. 499-505, 1959.

[7] P. Seiler, A. Pant and K. Hedrick, "Disturbance Propogation in Vehicle Strings," *IEEE Transactions on Automatic Control*, vol. 49, no. 10, 2004.

[8] S. Darbha and K. R. Rajagopal, "Intelligent Cruise Control Systems and Traffic Flow Stability," California Partners for Advanced Transit and Highways, 1998.

[9] J. Zhou and H. Peng, "String Stability Conditions of Adaptive Cruise Control Algorithms," in *IFAC symp.on "Advances in Automotive Control"*, 2004.

[10] P. A. Ioannou and C. C. Chien, "Autonomous intelligent cruise control," *IEEE Transactions on Vehicular Technology*, vol. 42, pp. 657-672, 1993.

[11] A. Kesting, M. Treiber and D. Helbing, "Enhanced Intelligent driver model to access the impact of driving strategies on traffic capacity," *Philosophical Transactions of the Royal Society A*, vol. 368, no. 1928, 2010.

[12] P. Barooah, P. G. Mehta and J. P. Hespanha, "Mistuning-based Control Design to Improve Closed Loop Stability Margin of Vehicular Platoons," *IEEE Transactions on Automatic Control*, vol. 54, no. 9, 2009.

[13] P. J. Zwaneveld and B. van Arem, "Traffic effects of automated vehicle guidance systems," Department of Traffic and transport, 1997.

[14] A. Kesting, M. Treiber, M. Schonhof, F. Kranke and D. Helbing, "Jam-avoiding adaptive cruise control (ACC) and its impact on traffic dynamics," in *Traffic and Granular Flow*, A. Schadschneider, T. Poschel, R. Kuhne, M. Schreckenberg and D. Wolf, Eds., Berlin,

Springer, 2005, pp. 633-643.

[15] C. Daganzo, "Requiem for second-order fluid approximations of trafficflow," *Transportation Research B*, vol. 29, no. 4, 1994.

[16] C. Daganzo, V. Gayah and E. Gonzales, "Macroscopic relations of urban traffic variables: Bifurcations, multivaluedness and instability," *Transportation Research B*, vol. 45, no. 1, 2011.

[17] D. Helbing and M. Shreckenberg, "Cellular automata simulating experimental properties of traffic flow," *Physical Review E*, vol. 59, no. 3, 1999.

[18] M. Treiber, A. Kesting and D. Helbing, "Understanding widely scattered traffic flows, the capacity drop, and platoons as effects of variance-driven time gaps," *Physical Review E*, vol. 74, no. 1, 2006.

[19] D. Helbing, M. Treiber, A. Kesting and M. Schonof, "Theoretical vs. empirical classification and prediction of congested traffic states," *European Physical Journal B*, vol. 69, no. 4, 2009.

[20] K. Jerath and S. Brennan, "Adaptive Cruise Control: Towards higher traffic flows, at the cost of increased susceptibility to congestion," in *Proceedings of AVEC 10*, Loughborough, UK, 2010.

[21] K. Nagel and M. Paczuski, "Emergent traffic jams," *Physical Review E*, vol. 51, no. 4, pp. 2909-2918, 1995.

[22] R. Mahnke, J. Kaupuzs and V. Frishfelds, "Nucleation in physical and nonphysical systems," *Atmospheric Research*, vol. 65, pp. 261-284, 2003.

[23] R. Mahnke, J. Kaupuzs and I. Lubashevsky, "Probabilistic Description of Traffic Flow," *Physics Reports*, vol. 408, 2005.

[24] R. Kuhne, R. Mahnke, I. Lubashevsky and J. Kaupuzs, "Probabilistic Description of Traffic Breakdowns," *Physical Review E*, vol. 65, no. 6, 2002.

[25] J. Schmelzer, G. Ropke and R. Mahnke, Aggregation Phenomena in Complex Systems, Wiley-VCH, 1999.

[26] R. Ackelik and D. C. Briggs, "Acceleration Profile Models for Vehicles in Road Traffic," *Transportation Science*, vol. 21, no. 1, pp. 36-54, 1987.

[27] G. Long, "Acceleration Characteristics of Starting Vehicles," *Journal of the Transportation Research Board*, vol. 1737, pp. 58-70, 2000.

[28] A. D. May, Traffic Flow Fundamentals, Prentice-Hall, Inc., 1990.

[29] B. Kerner and H. Rehborn, "Experimental Properties of Complexity in Traffic Flow," *Physical Review E*, vol. 53, no. 5, 1996.

Kshitij Jerath received the M.S. degree in mechanical engineering from The Pennsylvania State University in 2010. He is currently a Ph.D. candidate in the Department of Mechanical and Nuclear Engineering at The Pennsylvania State University. His research interests include dynamics and control of complex systems, networked control systems, intelligent vehicles and state estimation. His recent work has focused on developing terrain-based vehicle tracking algorithms for GPS-free and degraded GPS environments. He can be contacted at 336C Reber Building, University Park, PA 16802 or at kjerath@psu.edu.

Sean Brennan received his B.S.M.E and B.S. Physics degrees from New Mexico State University in 1997, and his M.S. degree and Ph.D. degree in Mechanical and Industrial Engineering at the University of Illinois at Urbana-Champaign, in 1999 and 2002, respectively. Since 2003, Dr. Brennan has taught at Penn State University where he is currently an Associate Professor in the Mechanical and Nuclear Engineering department. His research group is active in the areas of estimation theory, system dynamics, and control with applications focused primarily on mobile ground systems including passenger vehicles, heavy trucks, and bomb-disposal robots. He is currently an associate editor of the *Journal of Dynamic Systems, Measurement and Control*. He can be contacted at 157E Hammond Building, M&NE Department, Penn State, University Park, PA 16802. sbrennan@psu.edu .